ELSEVIER

Journal of Power Sources 109 (2002) 234–238

JOURNAL OF POWER SOURCES

www.elsevier.com/locate/jpowsour

Short communication

Cycling behavior of selenium-doped $LiMn_2O_4$ spinel cathode material at 3 V for lithium secondary batteries

C.S. Yoon, C.K. Kim, Y.-K. Sun*

Department of Materials Science and Engineering, Hanyang University, 17 Haengdang-dong, Seongdong-ku, Seoul 133-791, South Korea

Received 18 September 2001; accepted 15 January 2002

Abstract

Selenium-doped $LiMn_2O_4$ spinel cathode is synthesized by a sol–gel method. In spite of the observed Jahn–Teller phase transformation, the cathode exhibits a gradual gain in capacity when cycled in the 3 V range. Selenium-doped $LiMn_2O_4$ ($LiSe_{0.1}Mn_{1.9}O_4$ and $LiSe_{0.4}Mn_{1.6}O_4$) delivers 98 and 105 mAh g^{-1}, respectively, at a current density of 0.2 mA cm^{-2} in the voltage range of 2.4–3.5 V, without the capacity loss typically seen with unmodified spinel material in the 3 V range. Although, the exact mechanism for such capacity enhancement is not clear, it is proposed that the particle size and the structural distortion of the prepared powder may play a significant role in negating the volume change involved with Jahn–Teller phase transformation during cycling.

Keywords: Spinel; Chelating agent; Doping

1. Introduction

$LiMn_2O_4$ with a normal spinel structure ($Fd\bar{3}m$) has recently received much attention as a cathode material for lithium rechargeable batteries because of the low cost and non-toxicity of manganese [1–3]. Wide use of the material has been limited, however, due to the gradual degradation of its capacity on extended electrochemical cycling. The capacity fading has been attributed to a number of causes which include spinel particle dissolution in the electrolyte [4], the Jahn–Teller effect [2], and lattice instability [5].

In general, the discharge curve of the $Li \mid Li_xMn_2O_4$ cell exhibits two voltage plateaux. In the range $0 \leq x \leq 1$, the cell discharges at 4 V versus Li/Li^+, whereas when $1 \leq x \leq 2$, the cell discharges at 3 V versus Li/Li^+ [6,7]. Although, the 4 V voltage exhibits a relatively high specific capacity and power capability, the 3 V range suffers a large capacity fading on cycling due to Jahn–Teller distortion of the spinel lattice. The distortion is caused by Mn^{3+} ions and reduces the crystal symmetry change from cubic to tetragonal ($F4_1/ddm$) in $Li_2Mn_2O_4$ during lithium insertion. The transformation leads to a volume change that is sufficiently large to destroy the structural integrity of the material.

In order to improve the cycling performance of the spinel electrode in the 3 V range, several researchers have attempted to substitute a small fraction of the manganese ions with other metal cations. Partial substitution of Al, Cr, or Co for Mn in the $LiMn_2O_4$ spinel has been reported to suppress the Jahn–Teller distortion [8]. Amine et al. [9] have also reported that the Jahn–Teller transformation is not observed in the 3 V range with $LiNi_{0.5}Mn_{1.5}O_4$ powder prepared by a sol–gel method [9]. Although, the reported materials were successful in suppressing the phase transition, both materials encountered a gradual loss of capacity on cycling. More recent studies, however, have shown that Jahn–Teller distortion and concomitant capacity fading in the 3 V range can be completely suppressed by doping $LiMn_2O_4$ spinel with sulfur [10].

In this paper, we present the electrochemical cycling behavior of selenium-doped $LiMn_2O_4$ spinel which also does not exhibit a gradual capacity loss on cycling.

2. Experimental

Selenium-doped $LiMn_2O_4$ was synthesized by a sol–gel method using glycolic acid as a chelating agent. $Li(CH_3COO)\cdot H_2O$, $Mn(CH_3COO)_2\cdot 4H_2O$ and SeO_2 (reagent grade) were dissolved in an appropriate cationic ratio (Li:Mn:Se = 1.0:1.9:0.1 and 1.0:1.6:0.4) in distilled water. The resulting solution was delivered dropwise to a continuously stirred aqueous solution of glycolic acid. The pH of the solution was adjusted to be in the range 8.5–9.5 by adding ammonium hydroxide. The resultant solution was evaporated at 70–80 °C until a transparent sol and gel was

* Corresponding author. Fax: +82-2-2290-1838.
E-mail address: csyoon@hanyang.ac.kr (C.S. Yoon).

0378-7753/02/$ – see front matter
PII: S0378-7753(02)00054-X

obtained. The resulting gel precursors were decomposed at 500 °C for 10 h in air, and then calcined at 800 °C in air for 10 h, and flowing oxygen for 15 h. $LiAl_{0.2}Mn_{1.8}O_4$ was prepared similarly for comparison.

The selenium content of the powder after synthesis was determined by means of an inductively coupled plasma (ICP) spectrometer. For this purpose, the powder was dissolved in the dilute nitric acid.

The cathode for electrochemical cycling was prepared with 12 wt.% carbon black and 8 wt.% polytetrafluoroethylene (PTFE). The powder mixture was pressed on to an aluminum Exmet. For the anode, a thin lithium foil was used. The electrodes were cycled in an electrolyte made of 1:1 mixture (by volume) of ethylene carbonate (EC) and propylene carbonate containing 1 M $LiClO_4$. The charge–discharge cycle was performed galvanostatically at a current density of 0.2 mA cm^{-2} with cut-off voltages of 2.4–3.5 V.

A powder X-ray diffractometer (XRD; Rigaku, Japan) using Cu Kα radiation, a transmission electron microscope (TEM; JEM2010, JOEL, Japan) and a scanning electron microscope (SEM) equipped with an energy-dispersive X-ray spectrometer (EDS) were employed to characterize the microstructure and morphology of the powder before and after electrochemical cycling.

3. Results and discussion

The XRD patterns of the as-prepared powders showed that all the three powders had a cubic spinel structure with lattice parameters of 8.177, 8.186, and 8.217 Å for the $LiAl_{0.2}Mn_{1.8}O_4$, $LiSe_{0.1}Mn_{1.9}O_4$ and $LiSe_{0.4}Mn_{1.6}O_4$ powders, respectively. The ICP results indicated the Li:Se ratio to be only 0.0079 and 0.018 in the $LiSe_{0.1}Mn_{1.9}O_4$ and $LiSe_{0.4}Mn_{1.6}O_4$ powders after calcination. In addition, EDS analysis of the as-prepared powder failed to show any trace of Se within the accuracy of the technique. It is plausible that most of the selenium is lost during the calcination process at 800 °C, since selenium has a very low boiling point at 680 °C and SeO_2 can sublime at ∼340 °C [11]. Considering the absence of Se in the spinel lattice, $LiSe_{0.1}Mn_{1.9}O_4$ and $LiSe_{0.4}Mn_{1.6}O_4$ powders will be denoted hereafter as $LiSe_{0.01}Mn_{1.9}O_4$ and $LiSe_{0.02}Mn_{1.6}O_4$.

Electron micrographs of the as-prepared $LiSe_{0.01}Mn_{1.9}O_4$ and $LiSe_{0.02}Mn_{1.6}O_4$ powders are presented in Fig. 1(a) and (b), respectively. The micrographs show that the particle size becomes smaller and the size distribution becomes much narrower with increasing doping level of selenium. For example, the particle size of the 0.1 wt.% doped powder ranges from 0.1 to 1 μm, while that of the $LiSe_{0.02}Mn_{1.6}O_4$ powder centres sharply around 0.2–0.3 μm. Although, only trace amounts of Se are found in the powders, the doping process substantially alters the powder morphology. A TEM bright field image and electron diffraction patterns for as-prepared $LiSe_{0.02}Mn_{1.6}O_4$ powder are shown in Fig. 2. Analysis of the diffraction patterns reveal that some of

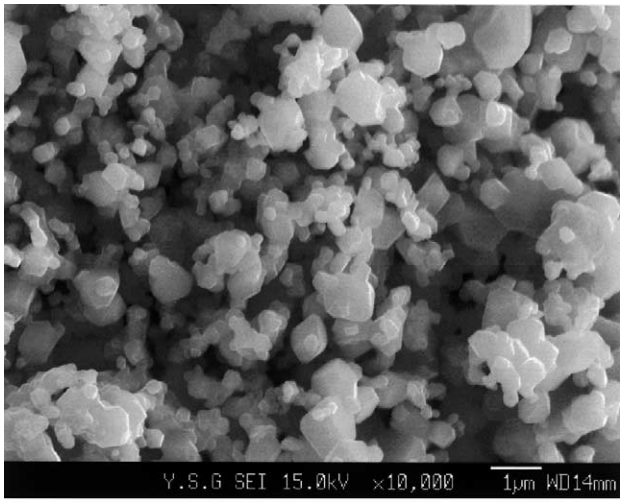

(a)

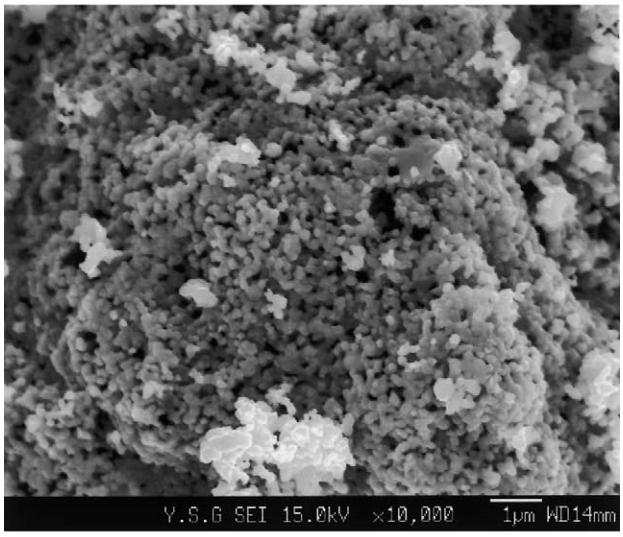

(b)

Fig. 1. Scanning electron micrographs of as-prepared powder: (a) $LiSe_{0.01}Mn_{1.9}O_4$; (b) $LiSe_{0.02}Mn_{1.6}O_4$.

the particles have a tetragonal structure, as indicated by the diffraction pattern in Fig. 2(c). Tetragonal $Li_2Mn_2O_4$ could have formed during the calcination process, as Se is lost through SeO_2 sublimination, which depletes the oxygen from the material. The oxygen deficiency can lead to the generation of Mn^{3+} (Jahn–Teller) ions that would result in the tetragonal transformation of the spinel phase [12]. Since XRD analysis is inherently biased towards larger particles, it is likely that tetragonal particles of sub-micrometre size do not show up in the XRD pattern due to line-broadening and the limited concentration.

Charge–discharge curves for $LiSe_{0.02}Mn_{1.6}O_4$, $LiSe_{0.01}Mn_{1.9}O_4$, and $LiAl_{0.2}Mn_{1.8}O_4$ powders when cycled between 2.4 and 3.5 V are given in Fig. 3. As previously reported [10], $LiAl_{0.2}Mn_{1.8}O_4$ suffers a significant loss in capacity. By contrast, both selenium-doped $LiMn_2O_4$ cathodes exhibit excellent cycleability; in fact, there is a noticeable increase in

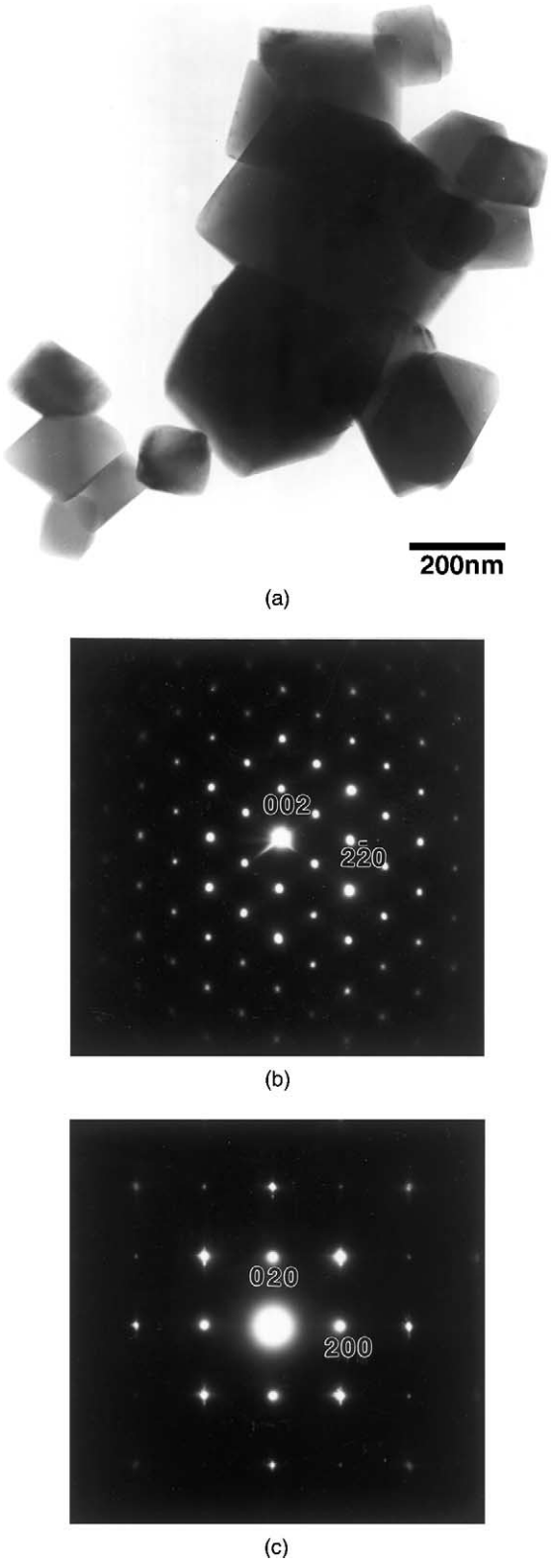

Fig. 2. (a) TEM bright field image of the $LiSe_{0.02}Mn_{1.6}O_4$ powder before cycling, (b) electron diffraction pattern of single spinel particle in (1 1 0) zone, (c) electron diffraction pattern of tetragonal particle in (0 0 1) zone.

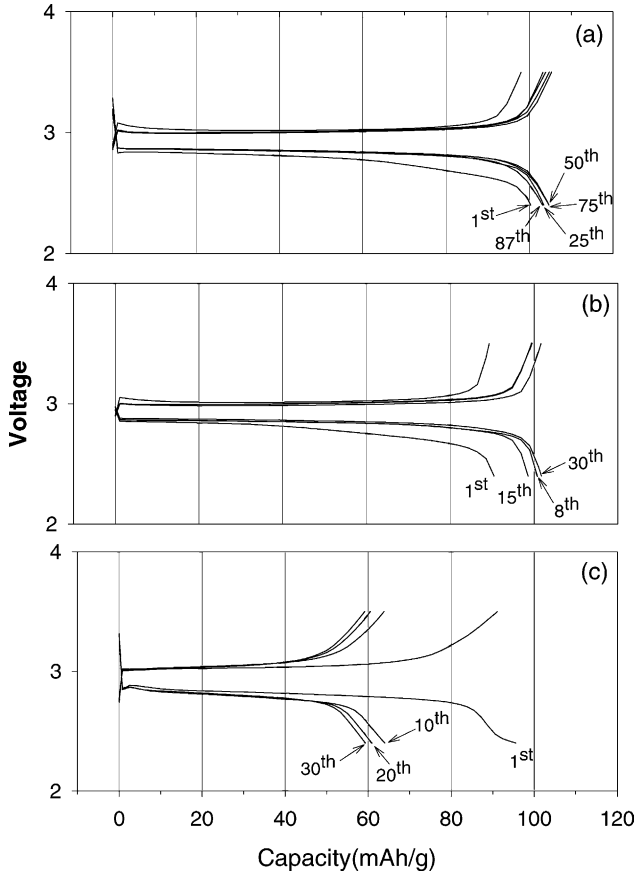

Fig. 3. Charge and discharge curves between 2.4 and 3.5 V: (a) $LiSe_{0.02}Mn_{1.6}O_4$, (b) $LiSe_{0.01}Mn_{1.9}O_4$, (c) $LiA_{0.2}Mn_{1.8}O_4$.

capacity after the first cycle. $LiSe_{0.01}Mn_{1.9}O_4$ and $LiSe_{0.02}Mn_{1.6}O_4$ deliver initial capacities of 89 and 100 mAh g^{-1}, respectively, that stabilize at increased capacities of 98 and 105 mAh g^{-1} after a few cycles. The flat voltage in all three curves suggests the existence of two phases which arise from the Jahn–Teller distortion [13]; yet, $LiSe_{0.01}Mn_{1.9}O_4$ and $LiSe_{0.02}Mn_{1.6}O_4$ powders show a capacity gain in spite of the apparent structural distortion.

The XRD patterns for the cathode powders (Fig. 4) show transformation of the cubic spinel phase to the tetragonal phase during cycling. An electron diffraction pattern of $LiSe_{0.02}Mn_{1.6}O_4$ after cycling is given in Fig. 5. This also confirms phase transformation during the charge–discharge process. Unlike the diffraction pattern in Fig. 2(c), the tetragonal pattern in Fig. 5 has split spots which indicate that the tetragonal particle after cycling has a distorted structure with several domains [14].

In comparison with the severe capacity loss shown by $LiAl_{0.2}Mn_{1.8}O_4$, Se-doping clearly suppresses the capacity fade which is known to be manifested by undoped $LiMn_2O_4$ spinel in the 3 V range. Both Al-doped and Se-doped $LiMn_2O_4$ undergo phase transformation; yet Se-doped $LiMn_2O_4$ maintains discharge capacity during cycling. The above results suggest that the Jahn–Teller phase

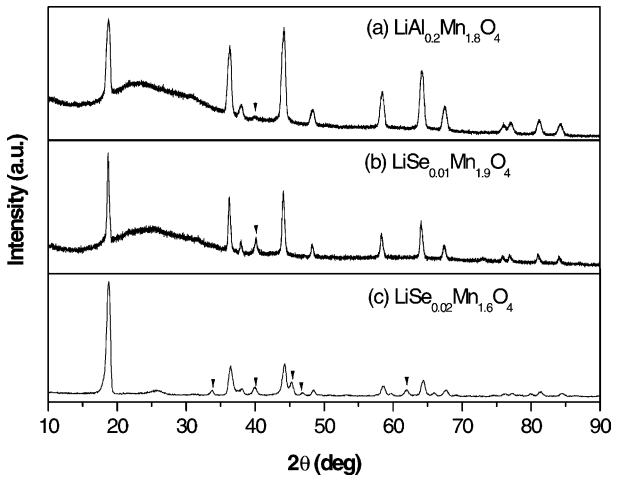

Fig. 4. XRD pattern for cathode powders after electrochemical cycling. Arrows indicate peaks from tetragonal phase: (a) $LiA_{0.2}Mn_{1.8}O_4$, (b) $LiSe_{0.01}Mn_{1.9}O_4$, (c) $LiSe_{0.02}Mn_{1.6}O_4$.

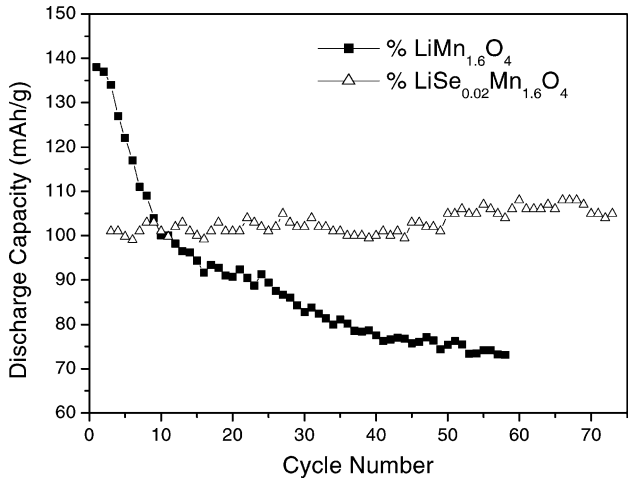

Fig. 6. Capacity curves for $LiSe_{0.02}Mn_{1.6}O_4$ and $LiMn_{1.6}O_4$ powders cycled between 2.4 and 3.5 V.

transformation may not play a significant role in electrochemical cycling at 3 V when the particle size is below a critical limit. Kang and Goodenough [13] also reached a similar conclusion by showing that a $LiMn_2O_4$ cathode, with a mean particle size of less than 0.8 μm, exhibited no capacity loss in spite of the tetragonal transformation at 3 V. Judging by the level of Se found in the as-prepared powder, Se atoms are not incorporated in the final spinel lattice, nor it is likely that Se atoms participate directly in the electrochemical cycling process. The small particle size appears to be a common observation when the spinel powder retained its capacity at 3 V in spite of the apparent phase transformation. It is concluded that as the particle size is decreased, the volume change involved with the tetragonal distortion becomes progressively insignificant. Also noted in the powders examined here is the existence of the initial tetragonal phase and the defective structure of transformed $Li_2Mn_2O_4$, although it is not clear whether the initial contamination has a direct bearing on the cycling behavior of the cathode.

Fig. 5. Electron diffraction pattern of $LiSe_{0.02}Mn_{1.6}O_4$ powder after cycling that shows transformed tetragonal phase in (1 0 0) zone.

To ascertain the effects of the Se-doping, we have also prepared a Mn-deficient spinel powder with a composition of $LiMn_{1.6}O_4$ under similar synthesis conditions. Unlike the $LiSe_{0.02}Mn_{1.6}O_4$ powder, $LiMn_{1.6}O_4$ showed definite capacity loss when cycled between 2.4 and 3.5 V. The capacity curves for both $LiSe_{0.02}Mn_{1.6}O_4$ and $LiMn_{1.6}O_4$ powders are presented in Fig. 6. Although we have not identified the exact mechanism of the capacity enhancement of the $LiMn_2O_4$ spinel cathode at 3 V, it is clear from Fig. 6 that selenium doping clearly alters the electrochemical properties of the spinel material. Investigations are underway to determine the initial structural difference between $LiSe_{0.02}Mn_{1.6}O_4$ and $LiMn_{1.6}O_4$ powders and to pinpoint the origin of the capacity enhancement caused by selenium doping from a microstructural point of view.

4. Conclusions

Selenium-doped $LiMn_2O_4$ powders have been synthesized by a sol–gel method using glycolic acid as the chelating agent. In spite of the Jahn–Teller induced phase transformation in the 3 V range, the Se-doped $LiMn_2O_4$ powder does not exhibit the rapid loss of capacity which is typically experienced with unmodified spinel powders. In fact, the doping appears to increase the capacity during cycling. Although, the exact mechanism for such capacity enhancement is not clear, it is suggested that the particle size of the prepared powder may play a significant role in negating the volume change involved with the Jahn–Teller phase transformation during cycling.

Acknowledgements

The authors wish to acknowledge the financial support received from the Hanyang University for this research.

References

[1] J.M. Tarascon, W.R. McKinnon, F. Coowar, T.N. Bowner, G. Amatucci, D. Guyomard, J. Electrochem. Soc. 141 (1994) 1421–1431.
[2] R.J. Gummow, A. de Kock, M.M. Thackerya, Solid State Ionics 69 (1994) 59–67.
[3] M.M. Thackery, A. de Koch, M.H. Rossow, D. Liles, J. Electrochem. Soc. 139 (1992) 363–366.
[4] D.H. Jang, J.Y. Shin, S.M. Oh, J. Electrochem. Soc. 143 (1996) 2204–2210.
[5] A. Yamada, J. Solid State Chem. 122 (1996) 160–165.
[6] J.M. Tarascon, E. Wang, F.K. Shokoohi, W.R. McKinnon, S. Colson, J. Electrochem. Soc. 138 (1991) 2859–2863.
[7] T. Ohzuku, M. Kitagawa, T. Hirayi, J. Electrochem. Soc. 137 (1990) 769–774.
[8] D. Song, H. Ikuta, T. Uchida, M. Wakihara, Solid State Ionics 117 (1999) 151–156.
[9] K. Amine, H. Tukamoto, H. Yasuda, Y. Fujita, J. Electrochem. Soc. 143 (5) (1996) 1607–1613.
[10] Sang Ho Park, Ki Soo Park, Yang Kook Sun, Kee Suk Nahm, J. Electrochem. Soc. 147 (6) (2000) 2116–2121.
[11] D.R. Lide (Ed.), Handbook of Physics and Chemistry, 73rd Edition, CRC Press, Boca Raton, FL, 1992.
[12] A. Yamada, K. Miura, K. Hinokuma, M. Tanaka, J. Electrochem. Soc. 142 (7) (1995) 2149–2156.
[13] Sung-Ho Kang, J.B. Goodenough, J. Electrochem. Soc. 147 (10) (2000) 3621–3627.
[14] L. Dupont, M. Hervieu, G. Rousse, C. Masquelier, M.R. Palacin, Y. Chabre, J.M. Tarascon, J. Solid State Chem. 155 (2) (2000) 394–408.